




Article

River Water Quality of the Selenga-Baikal Basin: Part II—Metal Partitioning under Different Hydroclimatic Conditions

Nikolay Kasimov ¹, Galina Shinkareva ^{1,*}, Mikhail Lychagin ¹, Sergey Chalov ¹, Margarita Pashkina ¹, Josefin Thorslund ² and Jerker Jarsjö ²

¹ Faculty of Geography, Lomonosov Moscow State University, 119991 Moscow, Russia; nskasimov@mail.ru (N.K.); lychagin2008@gmail.com (M.L.); hydroserg@mail.ru (S.C.); rita_pashkina.msu@mail.ru (M.P.)

² Department of Physical Geography and the Bolin Centre for Climate Research, Stockholm University, SE-106 91 Stockholm, Sweden; josefin.thorslund@natgeo.su.se (J.T.); jerker.jarsjo@natgeo.su.se (J.J.)

* Correspondence: galina.shinkareva@gmail.com; Tel.: +7-909-633-2239

Received: 4 July 2020; Accepted: 20 August 2020; Published: 26 August 2020



Abstract: The partitioning of metals and metalloids between their dissolved and suspended forms in river systems largely governs their mobility and bioavailability. However, most of the existing knowledge about catchment-scale metal partitioning in river systems is based on a limited number of observation points, which is not sufficient to characterize the complexity of large river systems. Here we present an extensive field-based dataset, composed of multi-year data from over 100 monitoring locations distributed over the large, transboundary Selenga River basin (of Russia and Mongolia), sampled during different hydrological seasons. The aim is to investigate on the basin scale, the influence of different hydroclimatic conditions on metal partitioning and transport. Our results showed that the investigated metals exhibited a wide range of different behaviors. Some metals were mostly found in the dissolved form (84–96% of Mo, U, B, and Sb on an average), whereas many others predominantly existed in suspension (66–87% of Al, Fe, Mn, Pb, Co, and Bi). Nevertheless, our results also showed a consistently increasing share of metals in dissolved form as the metals were transported to the downstream parts of the basin, closer to the Lake Baikal. Under high discharge conditions (including floods), metal transport by suspended particulate matter was significantly greater (about 2–6 times). However, since high and low water conditions could prevail simultaneously at a given point of time within the large river basin, e.g., as a result of on-going flood propagation, snap-shot observations of metal partitioning demonstrated contrasting patterns with domination of both particulate and dissolved phases in different parts of the basin. Such heterogeneity of metal partitioning is likely to be found in many large river systems. These results point out the importance of looking into different hydroclimatic conditions across space and time, both for management purposes and contaminant modeling efforts at the basin scale.

Keywords: metal partitioning; the Selenga River basin; Lake Baikal; water pollution; aquatic geochemistry

1. Introduction

Metals and metalloids (hereafter referred to as metals) are transported by river flow in dissolved and solid phases. The latter can be seen in the water column (suspended load) or near the bottom (bed load). The metal partitioning processes vary between different metals and metal complexes, for different river water conditions (e.g., pH, redox state and temperature [1]), and for different sediment conditions. The latter includes the fractionation of sediments, since different sediment fractions can sorb metals to different degrees [2–4].

In river waters, multiple complex factors govern metal partitioning, such as metal concentrations being subject to seasonal changes. The dominant form of metal transport by river flow also depends largely on the sediment availability and supply [5,6]. A strong correlation has been reported between the total suspended sediment content and the total heavy metal loads [7,8]. High sediment concentrations are typically observed during floods (e.g., [9,10]), reflecting higher contributions of soil erosion and river channel erosion [11–13].

Although a wealth of metal/water quality studies have contributed to a better understanding of various governing processes for river water quality, studies focused specifically on metal partitioning in river basins (Supplementary Material, Table S1) have mostly been based on local datasets within small catchments, or with a limited number of observation points (frequently just one) within large river systems [14–18]. In addition, there is a relatively limited number of studies that target different hydrological seasons [19–22]. Knowledge is therefore limited regarding metal transport under high flood conditions, including possible impacts of variability in hydroclimatic extremes within large river basins [23–25]. This contributes to the fact that the spatial variability of metal partitioning and its controls across scales remain unclear, although such variability may have significant impact on the basin-scale transport of metals.

For improved understanding of the mechanisms controlling the concentrations of metals in rivers, and to support the rigorous design of research and monitoring programs, time series datasets of dissolved and particulate metals in rivers are important. Such time series data are valuable for both historical flux and load calculations, and for future trend predictions [9,24,26]. Furthermore, in assessments of potential future changes in metal fluxes and loads, as a result of human pressures or hydroclimatic change, it is critical to understand how metals are partitioned in river waters under different ambient conditions [9,26]. This is because of the partitioning impacts the toxicity, mobility and bioavailability of metals.

Previous research on metal partitioning in the Selenga River basin was based mostly on single-season sampling campaigns and included heavy metal transport along the Mongolian part of the Selenga River watercourse [27], sediment-associated metal partitioning along the Selenga lowermost reach [28] and its delta [29], as well as metal spreading in the Selenga tributaries [30,31]. In this study, we present an extensive, novel dataset for the Selenga River basin—the largest tributary of Lake Baikal [32]—which is based on spatially distributed sampling locations that were visited during field campaigns over six years, from 2011 to 2016, to assess different hydrological seasons. It was reported that suspended sediment transport plays important role in total sediment budget within the Selenga River basin, and only in the very downstream part is it supplemented by bed load transport [33], which is why we focus here on water-suspended sediment partitioning and consider bed load transport being relatively low. The measurement and calculation of riverine water and sediment quality parameters are subject to significant statistical errors which should be evaluated when considering the study [34]. As concentration samples are usually infrequent (from weekly to monthly), only a minor part of the daily river flux is known, representing the first source of flux uncertainties [35]. Significant drifts in the measured quantities may arise due to the location of the sampling in the river section, because suspended sediment concentration varies within the river cross-sections, thus necessitating a series of depth- and width-integrated measurements [36]. Accuracy and precision of flux estimates depend on: (i) the type of river material (suspended particulate matter, nutrients), (ii) the sampling strategies and the reporting period [37,38], (iii) catchment characteristics such as basin size, and (iv) the role of transport regime [34,39]. In this study we relied on the previous above mentioned estimation of uncertainties and errors to minimize their effects on the results. The overall objective of this study is to utilize this high-resolution dataset for studying spatio-temporal patterns of metal partitioning and transport under different hydroclimatic conditions. Specifically, we aim to determine to what extent: (i) metal partitioning differs during high water and low water conditions, (ii) metal partitioning shows systematic differences in various sub-catchments of a river basin (e.g., depending on their upstream or downstream location), and (iii) the spatio-temporal patterns are specific to different groups of metals.

2. Materials and Methods

2.1. Study Area

The transboundary Selenga River is the main tributary of Lake Baikal, which has been a World Heritage Site since 1996. The Selenga River basin occupies 447,000 km² within the mountainous central part of the Asian mainland and stretches between 46°20' and 53°00' N and 96°50' and 112°50' E. The total number of rivers in the Russian part of the Selenga River basin is more than 17,000, with a total length of about 70,000 km. The geographical conditions of the Selenga basin are described in more detail in Part I [40].

The Selenga River basin can be divided into sub-catchments of large tributaries such as the Tuul, Kharaa, Orkhon, Dzhida, Chikoy, Khilok and Uda rivers, as well as smaller ones: Khan-gol, Eroo, Boroo, Temnik and others (Figure 1a). Anthropogenic activities within these watersheds have a significant impact on transport processes and metal migration. The anthropogenic pressures have been particularly high in the Mongolian part of the Selenga River basin, due to rapid urbanization [41–43], deforestation [44,45], gold mining [46,47], mining of other minerals, and grazing [48].

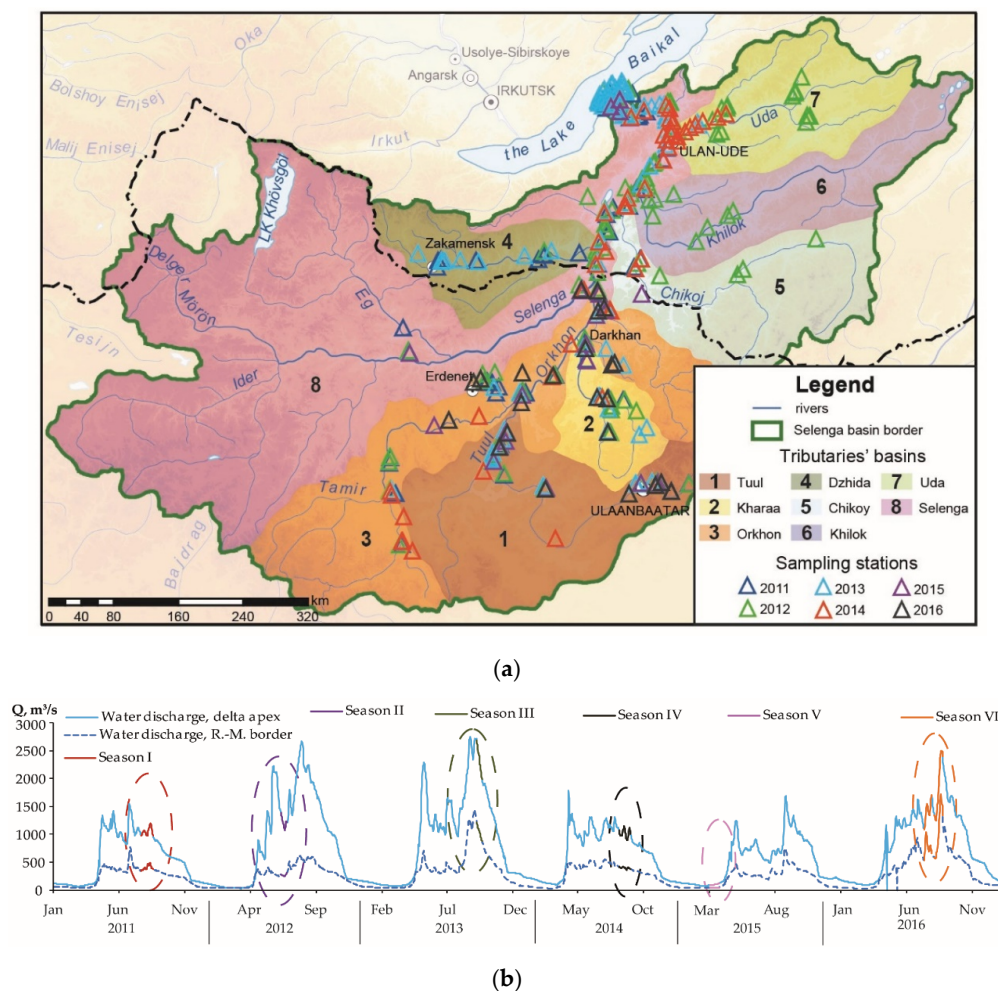


Figure 1. Field data acquisition: (a) sampling points, (b) water discharges of Selenga River delta apex and near Russian–Mongolian border.

For instance, the Tuul River basin contains the urban agglomeration Ulaanbaatar and the Zaamar gold field, and the Kharaa River basin contains the Boroo gold field deposit. These basins drain into the Orkhon River basin, which additionally contains a Cu–Mo mining and processing plant, located in the town of Erdenet. In the Dzhida River basin there is a large W–Mo mining and processing

plant. In the lower reaches of the Uda River basin the city of Ulan-Ude is situated, which is the capital of the Republic of Buryatia. Anthropogenic impact is manifested on various spatial scales: local—near cities, regional—as a result of hydraulic project implementation and the formation of extended anthropogenic flows in river waters, and global—as a response to climate change [49,50] and atmospheric pollution [32,51,52]. The spatio-temporal pattern of metal concentrations and partitioning, which is investigated here through direct observations, hence reflects combined effects of primary anthropogenic inputs (or source terms), and the redistribution of these inputs through transport and retention processes, including e.g., deposition and resuspension of contaminated river sediments, as well as sorption and redissolution of metals to river sediments.

2.2. Field Sampling, Analytical Procedures and Interpretation Methods

This paper summarizes a large dataset of dissolved and suspended metals, sampled throughout the Selenga River basin from 2011 to 2016. Field work was carried out at more than 100 sampling stations (Figure 1a), covering the following rivers in the Mongolian part of the basin; Selenga main branch, Orkhon, Khan-gol, Tuul, Kharaa, and Eroo. In the Russian part of the basin, the following rivers were covered: Selenga main branch, Dzhida, Chikoj, Khilok, and Uda. Additionally, the sampling campaigns covered different hydrological conditions of 2011–2016 (Figure 1b), which enabled characterization of high-resolved, spatial patterns of metal partitioning under contrasting hydrological conditions. Each sampling at a certain river was attributed to high-water (HW) or low-water (LW) conditions based on relative discharge, calculated as:

$$K_q = Q_i/Q_{i0}, \quad (1)$$

where Q_i is the locally measured discharge across the sampled section of river i during the considered field campaign; Q_{i0} is the average long-term annual discharge across the sampled section of river i , calculated based on the average runoff from the continuous monitoring at the Russian–Mongolian border (or at the delta apex when closer), with location-specific adjustments based on average regional water runoff (flow accumulation) maps [53]. When $K_q > 1$ the hydrological conditions are related to HW, and when $K_q < 1$ the conditions are related to LW.

Water samples were taken once at each sampling station in 2- and 5-L polyethylene terephthalate bottles in the mid-channel from the near-surface water layer. After sampling, each sample was filtered on a Millipore vacuum station with a Millivac Mini Vacuum Pump (230 v 50 Hz) through pre-weighted 47 mm membrane filters with a pore size of 0.45 microns to separate dissolved metal fractions from the suspended ones. The filters were then dried and reweighted to determine suspended sediment concentrations (SSC, mg/L). Grain size analysis of suspended sediments was conducted with the Laser Particle Sizer Fritsch Analysette 22. Furthermore, the average diameter of suspended sediments D_0 (mm) was counted. In practice, metals passing through a filter of 0.45 microns (μm) are conventionally called dissolved. In fact, this fraction consists of free ions, complex ions, metals bound to various ligands and other molecules with different chemical characteristics. These molecules can form larger compounds of both organic and inorganic genesis. Metals from suspended sediment samples that deposit on the filter are referred to as the suspended fraction. We did not further separate truly dissolved fractions from colloidal fractions as well as metals bound to suspended organic matter from those bound to minerals, as we focused on the total suspended and total dissolved metal concentrations. To preserve river water samples for metal analysis, conservation with 0.1 mL of HNO_3 (conc.) was performed.

Concentrations of As, B, Bi, Cd, Co, Cr, Cu, Fe, Mn, Mo, Ni, Pb, Sb, Sn, U, V, W, Zn) in dissolved (C_{diss} , $\mu\text{g/L}$) and suspended (C_{susp} , $\mu\text{g/g}$) forms were determined using ICP-MS and ICP-AES methods with the Elan-6100 and Optima-4300 DV («Perkin-Elmer», Waltham, MA, USA) instruments in the All-Russian Scientific-Research Institute of Mineral Resources, named after N.M. Fedorovsky in Moscow. This laboratory is accredited by the national accreditation system (RA.RU.21ГП11) as well as the international analytical system Accreditation (AAC.A.0025). It also complies with the requirements

of the International Standards ISO Guide 34:2009 and ISO/IEC 17025:2017. The calculation of the suspended metal share was made according to Equation (2) below:

$$C_{susp,\%} = 100\% \times C_{susp} \cdot SSC \cdot 10^{-3} / (C_{susp} \cdot SSC \cdot 10^{-3} + C_{diss}), \quad (2)$$

where $C_{susp,\%}$ is the share of suspended metal N (%), C_{susp} is the metal N concentration in suspended phase, ($\mu\text{g/g}$), SSC is the suspended sediment concentration (mg/L), C_{diss} is the metal N concentration in dissolved form ($\mu\text{g/L}$), and 10^{-3} is the conversion factor from milligrams to grams. To get general overview about metal partitioning patterns, we applied Principal Components Analysis (PCA) to the $C_{susp,\%}$ data set.

There are numerous methodological approaches related to substance partitioning under different conditions (Supplementary Material, Table S1). The partitioning coefficient (K_d) approach, which will be used in the present study, is the widely adopted one [5,54–56]. It is calculated as the ratio between the metal N concentrations in suspended matter ($\mu\text{g/L}$) and river water ($\mu\text{g/L}$). It assumes linearity between the suspended and dissolved metal concentrations, such that the ratio of suspended to dissolved metal concentrations is time-invariant under given geochemical conditions. Bed load was not studied in this manuscript, since the influence of bottom sediments on the composition of suspended sediments is rather insignificant within the Selenga River basin [53]. Moreover the content of metals in bottom sediments is generally lower than in suspended ones [53].

3. Results and Discussion

3.1. Trends of Seasonal Changes in Metal and Metalloid Partitioning

Based on the partitioning coefficient values (K_d), three main groups of metals emerged; group (1), termed “S-metals” ($K_d \geq 3$), were dominated by the suspended form and included Fe, Mn, Bi, Co, and Pb. Group (2) termed “D-metals” ($K_d \leq 0.1$), were dominated by transport in the dissolved form and included B, Sb, U, Mo. Finally, group (3), termed “S,D-metals” (with $0.1 < K_d < 3$), were defined as being most dependent on hydrological and anthropogenic factors, and included Ni, V, Cr, Cu, W, Sn, Cd, Zn, and As. Generally, S- and D-metals showed consistent partitioning patterns regardless of hydroclimatic variability in precipitation, water and suspended matter discharges, etc. However S,D-metals revealed significant differences in $C_{susp,\%}$ values between high and low water conditions (Supplementary Material, Table S2). This was shown by a flood in the Mongolian part of the Selenga River basin (HW conditions, $K_q > 1$ in all rivers) in July–August of 2011 (Supplementary Material, Table S2). This flood led to a sharp increase in the proportion of suspended Fe, Mn, Pb, Co, Bi, and Zn (>75% of the total content) as well as Ni, V, Cd, and Cu (50–75%). Furthermore, a large precipitation event (up to 35 mm) in the Orkhon River basin, which caused intensive soil and bank erosion, increased the proportion of suspended forms of all metals (except for Mo and Sb), and also generally enriched the metal content of suspended particles. Even for As and U, which are commonly dominated by the dissolved phase, riverine suspended transport became predominant (up to 70–79%) during this high flow event. At the same time, downstream parts of the Selenga River basin (in Russia) were characterized by low water conditions (LW conditions, $K_q < 1$ in all rivers), with predominantly dissolved forms of all metals. The only exception to this trend was observed for W, which mainly originate from the tailings of the Dzhidinsky mining and processing plant in the Zakamensk town, from where it enters the aquatic systems predominantly in suspended form.

Another spatial pattern of metal partitioning was revealed in June–July 2012. Most of the rivers in Mongolia with a few exceptions (Boroo, Khara and Tuul rivers) were characterized by a summer low water period (LW). Low suspended sediment concentrations in the Selenga River basin caused a tendency to a predominance of the dissolved fraction for all metals except Fe, Mn, Co, Bi, V, and Cr (Supplementary Material, Table S2). The largest portion of dissolved forms was found for W, Sn, U, and Mo. In some rivers summer rains induced fast floods, especially in the Dzhida River where daily rainfalls over 15 mm were observed during a week. This caused an increase in As, Zn, and

Cd in suspended form. Similar observations were made under HW conditions in the Boroo River, Mongolia. In the Dzhida River over 85% of Fe, Mn, Pb, Co, Bi, Ni, V, Cu, Cr and 60% of As and Cd were transported by suspended particulate matter. Furthermore, intensive precipitation in the Kharaa River basin (about 20 mm) provoked an increase in the proportion of suspended forms of metals: up to 78% for Bi, 53–64% for Fe, Mn, Co, Cr, V.

Observations from September 2013 demonstrate conditions of flood recession throughout the whole Selenga River basin. Even though the precipitation was rather low during this month, most of the rivers were characterized by HW conditions. For example, the middle reaches of the Kharaa and Khan-gol rivers during sampling period received about 5.1 and 6.1 mm of precipitation, respectively, and the upper reaches of the Eroo River received about 12.2 mm. Dissolved forms remained predominant for B, Mo. With single exceptions, dissolved forms were also predominant for U, Sb, As, and Zn (Supplementary Material, Table S2). The share of suspended forms of Fe, Mn, Pb, Co, and Bi exceeded 75% in most tributaries. For Ni, V, Cu, Cr, and Sn the share was 50–75%. In the Khan-gol River as well as the Tuul River downstream of the Zaamar goldfield metals were largely transported by the suspended particulate matter. This could be explained by a combination of anthropogenic factors—e.g., gold mining in Zaamar, the mining and processing plant in Erdenet in the Khan-gol basin, and natural factors—e.g., high pH due to geological conditions [31], increased precipitation and intensification of bank erosion processes. In particular, the sediment budget of the mine-affected Tuul River is dominated by in-channel sources during flood events [57] that have a higher proportion of carbonate inputs, which are less contaminated by metals. For the Russian part of the Selenga River basin, the observed prevalence of suspended forms in Chikoy River is mainly due to natural factors—sampling was done after significant floods related to precipitation events of up to 18.7 mm.

Another example of less heterogeneous hydrological conditions was revealed during August of 2014 in the Russian part of the Selenga River basin, when the summer flood recession was impacted by minor rainfall events (HW and LW conditions prevailed at the same time in different rivers). Under these conditions, the share of suspended metals decreased compared to the other seasons (Supplementary Material, Table S2). For all the studied tributaries Fe, Mn, and Co were largely transported by the suspended particulate matter (>82%) with the exception of the Khilok River.

A homogenous metals partitioning pattern dominated by dissolved forms (except Fe, Ni, and Pb; Supplementary Material, Table S2) can be seen during winter LW conditions (March 2015), when the river system is covered by ice, as it is then fed mostly by sediment-free ground water. The amount of suspended solids in the rivers of the Selenga River basin was then less than 3 mg/L with a few exceptions. Notably, in the Tuul River downstream of Ulaanbaatar city untreated wastewaters increased suspended sediment concentrations up to 312 mg/L. In particular, since the river froze completely upstream of the city, the river flow downstream of it almost entirely consisted of wastewater, which caused a significant increase in suspended forms of all metals (>53% for of all metals except U and Mn). Elevated suspended sediment concentrations could be distinguished more than 20 km further downstream near Lun' town (26 mg/L). This highlights the large-scale impact of local anthropogenic activities during low flow conditions.

Again, the impact of rainstorms during summer season was reflected in the partitioning pattern of July–August of 2016 (HW conditions). Increases in the share of suspended forms of all metals (Supplementary Material, Table S2) were observed. A high proportion of dissolved forms was found only for U, Mo, Sb, and As. During the field sampling campaign the maximum rainfall of the year (53.1 mm) was recorded in the Khara River basin. Heavy precipitation occurred also in the Khan-gol (27.4 mm) and Orkhon (10.7 mm) basins.

3.2. Metal Partitioning in Sub-Catchments throughout the Selenga Basin

During each hydrological sampling period the situation in different parts of the Selenga basin was not uniform. For instance, heavy precipitation in some small basins typically caused an increase in the suspended sediment concentration. Together with intense anthropogenic impact this led to an

increase in the share of suspended forms of metals (Figure 2). In the following, we will focus on the metal partitioning patterns in the most significant Selenga sub-catchments (Figures 1a and 2).

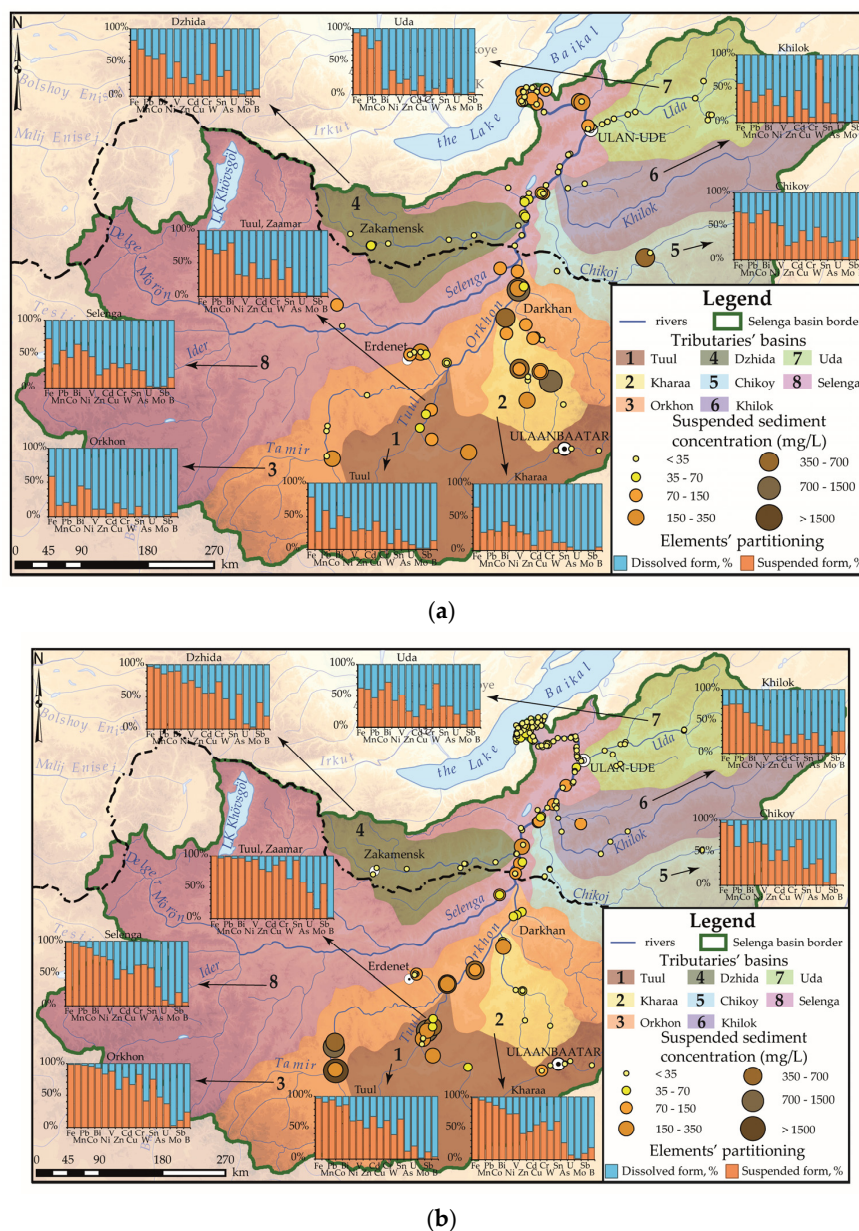


Figure 2. Metal partitioning and suspended sediment concentration during (on average): (a) low water period, (b) high water period.

3.2.1. The Tuul River Basin

The main sources of contamination within the Tuul River basin (Supplementary Material, Table S3; Figures 1a and 2, #1) are the Ulaanbaatar city in the upper reaches of the river and the Zaamar gold mining area more than 300 km further downstream. There are different pollutant sources in the Ulaanbaatar area [58]: the wastewater treatment plants at Nalaikh and Nisekh, the central wastewater treatment plant in Ulaanbaatar, bio-industry (for ex. chicken farms) and bio-Songino (livestock medicine factory and wastewater treatment plant). Wool and cashmere processing factories and tanneries which are concentrated in the floodplain of the Tuul River produce a significant amount of metals and toxic substances [59]. However, some of these factories have wastewater treatment plants. The gold mining of Zaamar occurs in three main ways: scrubber, sluice, and dredge mining. Of these, dredging has the greatest impact on water quality and metal concentrations, and sluice

has the least [60]. In the Zaamar placer gold mining area a bucket-line dredge and washing with pressurized water spraying are used [61].

On average, relative to the low water periods of the Tuul River, the flood periods and their recession (in the summers of 2011, 2013 and 2016) were associated with a significant increase in the share of suspended metals (Figure 2, Supplementary Material, Table S3), especially for Mn, Fe, Pb, and Bi (up to 84–100%). A main reason was an intense input of fine dust particles (0.001–0.005 mm) with the surface runoff pulse and resuspension of bottom sediments fine fraction. It was reported [61] that the suspended sediment concentrations of the Tuul River is often high during the summer months when mining is active. During the winter season after the closure of mining, the suspended sediment concentration is usually much lower. This corresponds to our data of maximum SSC values equal to 2,384 mg/L during the high water period (Figure 2b, Supplementary Material, Table S3) within the Zaamar mining area and 8.3 mg/L during winter low water period. Fe, Pb, Zn, As, and Cu are often associated with sulfide minerals (pyrite FeS₂, galena PbS, sphalerite ZnS, arsenopyrite FeAsS, chalcopyrite CuFeS₂) presented in metallic ore mining areas [61] and could also enter the rivers with weathering products of Archean granites and alluvial Quaternary sediments.

During the summer low water period of 2012 and winter low water period of 2015, the proportion of suspended metals as well as mean SSC values generally decreased (Figure 2, Supplementary Material, Table S3) in comparison with high water periods. However, in the winter downstream the city of Ulaanbaatar, it increased significantly compared to the upstream river part, due to the influence of the city's wastewater [62–64]. Thus, the suspended forms of Pb and Bi increased almost up to 100%; Cd, Cr, Zn, Sn, Cu, Fe, W, and V up to 82–99%; Co, Sb, Ni, As, and Mo up to 53–70%; and Mn and U up to 20%.

It is known that at high pH metals can transform into slightly soluble higher oxides, hydroxides and carbonates, which leads to a decrease in the proportion of dissolved forms and an increase in suspended forms [65]. Upstream of Ulaanbaatar city, the river is fairly clean, and within the city there is a sharp increase in pH value (from 7.6 to 9.4) and pollutant concentrations, the main source of which is the city's central wastewater treatment plant. According to Dalai and Ishiga [66] high concentrations of As, Pb, Zn, Cu, Ni, Cr, and V were found in the bottom sediments within the city. Cu, Cd, and Ni can enter aquatic systems with atmospheric deposition from coal combustion [67]. Mo, U, W, Sb, and As are common for ash of the city's thermal power station [68]. Zn, Mo, Cr, Cd, Pb, and Cu originate from vehicles [69] and accumulate in the soils of the city's transport zone [70].

During the flood recession of the 2013 field season, precipitation was not as abundant as during the 2011 field season. A significant increase in the share of suspended metals was then found downstream of the Zaamar gold field. An increase of 60–70 times was observed for Zn and Cd, 43 times for U, 21–28 times for Bi, W, Cr, and Mo, 13 times for As, and 4–5 times for Cu, V, and Co. This sharp increase in the suspended metals proportion can be explained by a significant suspended sediment concentration increase (650 times) in the Tuul River water from 4 mg/L far upstream to 2,384 mg/L downstream of Zaamar (Figure 2b) as a result of an intensive erosion of tailings stored along the banks of the river within the gold mining area and resuspension of fine particles due to dredging. An increase in the total riverine metal fluxes, especially Al, As, Cu, Fe, Mn, Pb, and Zn by 44, 30, 66, 48, 1.5, 76 and 65 tonnes per year, respectively, below Zaamar was also noted [71].

The summer season of 2016 (July–August) is characterized by rather high shares of suspended forms of not only Mn, Fe, Pb, and Bi which are typical for Tuul basin but also of Cr and Sn. The seasonality in total and dissolved concentrations of Al, As, Cu, Fe, and Mn in the Tuul River basin were identified earlier [71]: dissolved concentrations were shown to be significantly higher during June and July than in October. Significant differences between the dissolved and total concentrations were attributed to the domination of suspended heavy metals [71]. This fact correlates with our results for Mn, Fe, and Cu.

Thus, the influence of the Ulaanbaatar city on metal partitioning in the Tuul River aquatic systems is reflected in an increase in the share of suspended Cr, Ni, Pb, Mn, Co, Cu, Zn, and Cd up to 30–80% and dissolved Ni, B, and Cu up to 50–80% during the summer low water period. During flood events

downstream of Zaamar the share of all metals in suspended form increase because of intensive erosion of mining tailings and resuspension of particles due to dredging.

3.2.2. The Kharaa River Basin

The Kharaa River (Supplementary Material, Table S4; Figures 1a and 2, #2) experiences significant anthropogenic pressure due to the gold mining activities in the basin of its tributary—the Boroo River. Within the Boroo gold mining area high concentrations of Al, As, Cu, Mn, Fe, Pb, U, and Zn were found in river water [72], while waste waters of the tailings are enriched with As and Cu [73]. High As concentrations were determined in the ash basins of the Thermal Power Plant in Darkhan, from where with intense rainflow, resuspended ash can get into river waters. During floods period As, Pb, Zn, Ni, Fe, and Mn could feed into the river channel from groundwater downstream of the gold mining area, where high concentrations of these elements are found [74]. In the lower and middle reaches of the Kharaa River groundwater pollution with B and chlorides by domestic and industrial wastewater was detected [74].

Kharaa is characterized by a predominance in the dissolved fraction of As, U, Mo, Sb, and B (Figure 2; Supplementary Material, Table S4). It was found that the main source of suspended solids in the riverbed is the bank erosion (74%) [75]. Downstream of the confluence of the Boroo and Kharaa rivers, the SSC in the latter increases 11–45 times (Figure 2). The fraction of suspended Zn increases as well (18–26 times), along with Cu (2–4 times), Cr (5–170 times), and As (9–98 times). A significant increase in the proportion of suspended metals in low reaches of Kharaa River is associated with placer gold mining in the Boroo River basin, as well as an increase in the area of agricultural land use and in the number of livestock in the basin [76]. An expansion of the area of degraded land led to higher input of small suspended particles (0.001–0.01 mm) enriched with metals into the river channel [77,78]. In 2011 and 2016 sampling coincided with the maximum amount of precipitation (89.9 and 53.1 mm respectively), which led to significant floods and an increase in the proportion of suspended metals in river waters due to erosion and resuspension processes (Supplementary Material, Table S4).

3.2.3. The Orkhon River Basin

In the summer of 2011, studies in the Orkhon River basin (Supplementary Material, Table S5; Figures 1a and 2, #3) were carried out at the peak of a flood [56,79], which caused high SSC values (115–1459 mg/L). After the rains, the silt fraction (<0.001 mm) in suspended sediments increased from 5% to 31%, and all metals were predominantly found in suspended form, except the active water migrants Mo, Sb, and B (Figure 2a). During the high water season of 2016, a predominance of suspended metals fraction was also found in the main channel of the Orkhon River (Figure 2b; Supplementary Material, Table S5). It is associated with the episodes of precipitation that occurred during the sampling period, which caused an increase in the inflow of metals in suspended form due to activation of erosion and resuspension processes.

During the low water period of 2012, downstream of the confluence with Tuul River, an input of silt particles from Zaamar gold mining area contributed to a sharp increase in suspended Cr by 170 times, of As and Zn by 20–25 times, of Be, U, V, Cd, and Ni by 7–11 times, and of Pb, Co, Al, Mo, Fe, B, Mn, Cu, and Sn by 2–5 times, in comparison with the suspended metal concentrations of the upper reaches of the Orkhon River. During the flood recession conditions of 2013, the ratios of dissolved and suspended metals along the river varied slightly, increasing after the confluence with the Tuul River, along with a 17-fold increase in suspended sediment concentration. It is known that at the confluence points between the tributaries and the main river SSC values can be especially affected by resuspension processes [27]. Thus, the proportion of suspended Sb increased by 105 times, of Zn by 60 times, and of Cd, As, and Cu by 10–16 times. During the winter low water period of 2015, the proportion of suspended metals significantly decreased due to a decrease in the SSC values in the ice-cover period.

Thus, the influence of placer gold mining, which is conducted in the Tuul River basin and entails significant processing of watercourse beds in the vicinity of the Zaamar town [71], was reflected in the

Orkhon River as a sharp increase in suspended sediment concentration and suspended metal fractions further downstream (Figure 2; Supplementary Material, Table S5).

3.2.4. The Dzhida River Basin

Main sources of pollutants in the Dzhida basin (Supplementary Material, Table S6; Figures 1a and 2, #4) include the mine water of the closed Dzhidinsky W–Mo mining and processing plant and erosion of its tailings in the Zakamensk town. Furthermore, the soils of the industrial zone are enriched with Bi, W, Cd, Be, Pb, Mo, Sb, Cu, Zn, Sn, and As [80]. Dzhida waters are characterized by a higher suspended fraction of some metals during the low-water period (Figure 2; Supplementary Material, Table S6). The river has the highest concentrations of coarse dust particles in suspension (66% of particles with a diameter of 0.01–0.05 mm) compared to other tributaries of the Russian part of the Selenga basin. In the lower reaches of the river during floods, the proportion of suspended Cu and Co increased by 4 times, and Cd increased by 4–17 times as compared to the upper reaches. Compared to the high water period, the low-water period concentrations of Zn and As increased by 10–11 times. In addition to Zakamensk, the Sanginsky and Bayangolsky brown coal deposits are situated in the Dzhida basin [81]. Those deposits could be actively eroded by rainfall due to their fracturing [82].

The anthropogenic impact of Zakamensk and the erosion of the Dzhidinsky tailings in the flood of 2011 (August) can be traced all the way to the lower reaches of the Dzhida, decreasing the pH values to 6.9 and increasing the proportion of suspended forms of Al, As, B, V, Fe, Cr, Mn, Co, Sn, and U relative to the upstream river part. In the summers of 2012 and 2016 a significant increase in the SSC values and share of suspended forms of all metals, compared to low water periods, was found (Supplementary Material, Table S6), especially for ore-related Zn, Cr, and Fe. So, the predominance of suspended W, Co, Mn, and Fe and dissolved Mo is characteristic for Dzhida.

3.2.5. The Uda River Basin

The Uda River basin (Supplementary Material, Table S7; Figures 1a and 2, #7) experiences anthropogenic stress associated with the influence of the Ulan-Ude city [21], located at its mouth (Figure 2; Supplementary Material, Table S7). From the upper reaches of the river to the mouth, fluctuations in the share of suspended metals forms are insignificant: the share of Cr, Ni, As, U in the river suspension increases by 2–3.5 times.

During the low water period of 2012, most of the metals were found in dissolved form (Figure 2a), entering the aquatic systems mainly with wastewater from the Ulan-Ude city. In the recession of summer floods of 2013–2014, metals dominated in suspended form, which is most actively manifested by the example of Fe, Mn, Co, and Pb (Figure 2; Supplementary Material, Table S7). Rather high concentrations of W, Cu, Mo, As, Sb, Pb, Bi, Cd, Co, and Ni in bottom sediments within Ulan-Ude city were found near oil depot “Buryat-terminal” [83]. During the summer floods of 2011 the resuspension of contaminated bottom sediments could be the reason for increased proportions of suspended Fe, Mn, Co, Bi, and W in the lower reaches of the Uda River (Figure 2b).

3.2.6. Selenga Main Channel

In the Mongolian part of the Selenga basin (Table 1; Figures 1a and 2, #8), the suspended form of metal migration predominated, which is explained by the large amount of precipitation in the Mongolian territory during the sampling period. In the Russian part of the basin, in comparison with the Mongolian, the share of suspended As, U, and Mo increased by 2–15 times due to the erosion of the soils of industrial zones and tailings dumps in Zakamensk town. During floods, the intensity of surface washout and resuspension processes increased, which entailed an increase in the suspended forms of all metal proportions on average by 2–6 times. This was especially pronounced during the rain floods in July 2016, e.g., for of Zn, Cd, Cr, and V (Table 1). It was reported that Cd and Zn levels are highly correlated with organic content of the sediments [84].

Table 1. Metal partitioning in the Selenga River (median values).

Season & Year	SSC, mg/L		D ₀ , mm		100–75%	75–50%	50–25%	<25%	
	Max	Mean	Max	Mean					
Selenga Average	LW ₁₁ n = 32	117	28	0.11	0.07	Bi ₈₅ W ₈₀	V ₇₃ Co ₆₄ Fe ₆₀ Cd ₅₁ Pb ₅₀	Mn ₄₉ Ni ₄₀ Cu ₃₂ Sn ₃₀ Cr ₂₆	Zn ₂₁ As ₂₀ B ₆ U ₃ Mo ₁ Sb _{0,6}
	LW ₁₂ n = 40	242	56	0.05	0.03	Bi ₈₀	Fe ₆₃ Co ₆₀ V ₅₉ Cr ₅₇ Mn ₅₄	Pb ₄₉ Cr ₄₁ Ni ₄₀ As ₃₅ B ₂₆	Zn, W ₂₂ Sn ₂₀ Cd ₁₉ U ₆ Mo ₃
	HW ₁₃ n = 46	93	28	0.15	0.04	Fe ₉₈ Mn ₉₇ Co ₈₅ Pb ₈₃	Bi ₇₄ Ni ₆₀ V ₅₅	Cu ₄₀ W ₃₆ Cr, Sn ₃₅ Zn ₃₂ Cd, As ₃₁	Sb ₁₅ U ₇ B ₆ Mo ₂
	HW ₁₄ n = 67	49	20	0.68	0.10	Fe ₉₉ Mn ₉₆ Pb ₉₂ Co ₈₇ Ni ₈₅	Bi, W ₆₆ V ₆₄ Cr ₅₄	Cd ₄₆ Sn ₄₄ Cu ₄₀	As ₂₂ Sb ₁₉ Zn ₆ U ₄ Mo ₁ As ₂₂ Zn ₁₆ Cd ₁₅
	LW ₁₅ n = 17	9	2	0.05	0.04	Fe ₉₄ Ni ₈₄	Pb ₆₇	Cu ₃₇ Sn ₃₂ Bi ₂₈	Co ₁₁ Cr, V ₇ W, Sb ₆ Mn ₄
	HW ₁₆ n = 7	110	78	0.10	0.07	Fe ₁₀₀ Mn, Cr, Pb ₉₉ Co, Sn ₉₆ V ₉₄ Bi ₉₃ Cd ₉₀ W ₈₉ Zn ₈₇ Ni ₈₂	Cu ₆₈	As ₃₆ Sb ₂₉	U ₁₆ Mo ₄
Selenga delta	HW ₁₁ n = 15	71	21	–	–	W ₈₅ Bi ₈₄	V ₇₂ Co ₆₄ Fe ₆₀	Pb ₄₉ Mn ₄₈ Cd ₄₇ Ni ₃₉ Sn ₃₁ Cu ₂₇	Zn ₂₄ As, Cr ₂₂ B ₆ U ₄
	LW ₁₂ n = 19	199	59	0.02	0.02	Bi ₈₇	Cr ₆₉ V, Co ₆₅ Fe ₆₃ Mn ₅₆ Pb ₅₁	As ₄₈ Ni ₄₂ W ₃₅ Cu ₃₂ B ₃₀ Zn ₂₉ Cd ₂₅	Sn ₂₃ U ₈ Mo ₄
	HW ₁₃ n = 26	52	26	–	–	Fe ₉₈ Mn ₉₇ Pb ₈₇ Co ₈₅	Bi ₇₄ Ni ₅₈ V ₅₅	Cd ₄₅ Cu ₄₀ Zn ₃₇ W ₃₆ Cr ₃₅ Sn ₃₃ As ₃₁	Sb ₁₅ U ₇ B ₆ Mo ₂
	HW ₁₄ n = 52	43	19	0.68	0.11	Fe ₉₈ Mn ₉₅ Co ₈₆ Pb ₈₅ Ni ₈₄	Bi ₆₆ W ₆₄ V ₆₃ Cr ₅₃	Sn ₄₃ Cd ₄₂ Cu ₃₉	As ₂₂ Sb ₁₉ U ₄ Zn ₃ Mo ₁
	LW ₁₅ n = 12	9	2.3	0.05	0.04	Fe ₉₄ Ni ₈₉	Pb ₆₉ Sn ₅₁	Cu ₃₇ Bi ₃₄ As ₂₇	Cd ₂₄ Co ₁₉ Zn ₁₇ Sb, V ₉ Cr ₈ W ₇

SSC—suspended sediment concentration, HW—high water season, LW—low water season, subscript indicates sampling year, D₀—the average diameter of suspended particles. The cell color and the subscript of metal indicate the share of the suspended metal form (%).

Thus, during the period of the rain floods recession (September 2013), the proportion of the suspended form of metals increased in all considered basins by 2–6 times. The smallest influence of hydrologic and climatic conditions on the metal partitioning was characteristic of the Khilok and Chikoy river basins (Figure 2). The prevalence of the dissolved metals in the aquatic systems of these basins was quite stable and was associated with the absence of large sources of anthropogenic impact. In the Dzhida River basin, the influence of a large Cu–Mo mining and processing plant in Zakamensk town was manifested in a 2–8-fold increase in the proportion of suspended forms of all metals compared to the basins of other tributaries of the Russian part of the Selenga basin (Figure 2). Even during the summer low-water period (2012) suspended forms of metals were dominant, which was especially noticeable in an example of ore-related Cu, Zn, Ni, Cr, and As.

The Mongolian part of the basin was distinguished by an increased proportion of suspended metals compared to the Russian part (Figure 2), regardless of the amount of precipitation and hydrologic conditions, which are caused by high SSC values in it as a whole [85]. A larger proportion of suspended metals in comparison with the Russian part were determined for Al, Fe, Ti, Mn, Pb, and Co. These metals, together with a large amount of suspended material, enter the aquatic systems of the Tuul and Kharaa basins due to the gold mining (dredging) at Zaamar and Boroo. As, B, U, and Mo dominated in dissolved form in the Mongolian part of the basin. The tributaries of the Russian part of the Selenga basin were characterized by the predominance of dissolved forms in metal partitioning (Figure 2; Table 1), since this part is mostly a flat plain, which contributes to a decrease in flow rates and the deposition of fine suspended particles enriched with metals.

In the Selenga delta, the metal partitioning distribution changed slightly during the year, which is associated with intra-annual redistribution of discharge among the channels of the delta, a decrease in the hydrodynamic activity of the flow in comparison with upstream reaches, and the deposition of a significant part of suspended sediments in the floodplain and in the delta channels [29,36]. Thus, the share of the dissolved Mo and Cd in the delta reached up to $\geq 90\%$, whereas As, Cu, and Ni reached up to 30–50%, and the remaining metals reached up to $< 30\%$ (except for Cr and Pb).

3.3. Main Drivers of Metal Partitioning

The overall results indicate that flow conditions have defined grain size distribution which in turn played important role in controlling the spread of metals in suspended sediments, which is in line with findings of other studies [86,87]. The particle size distribution of the sediments was found to be significantly different during LW and HW conditions, with a two-fold increase in the number of particles smaller than 10 μm during HW conditions, due to surface erosion and decomposed organic matter in the runoff. Additionally, the spatial variability of metal partitioning is largely related to variations in sediment composition due to the impact of hot spots (mainly mining and urban areas). A case study of the Tuul River (Figure 3) clearly shows the transverse patterns of sediment composition due to the impact of the Ulaanbaatar city and Zaamar mining activities. The order of magnitude changes in sediment grain size even within a single season can largely explain the observed spatio-temporal variations in metal partitioning. The most important “ $< 10 \mu\text{m}$ ” fraction (i.e., clay-sized material), containing relatively high amounts of metals was considerable in Tuul River, accounting for approximately 20–40% of the suspended sediment load.

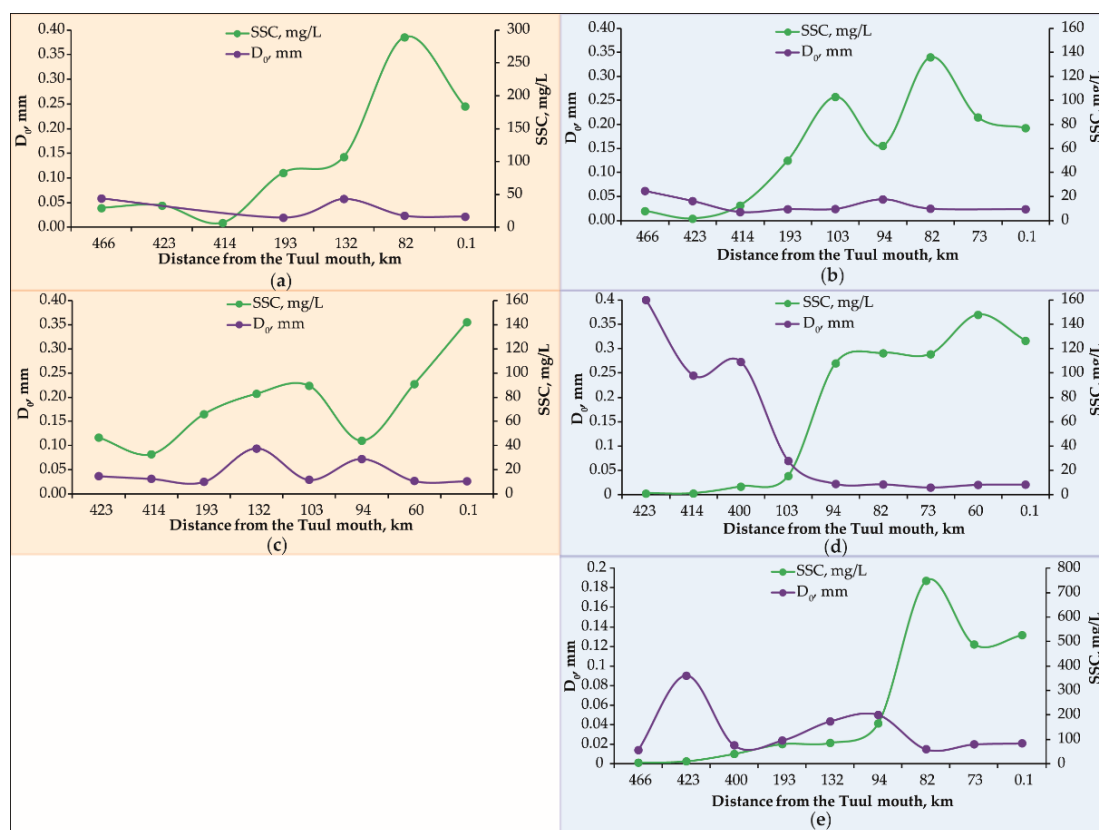


Figure 3. Suspended sediment concentrations (SSC) and grain size along Tuul River in different hydrological seasons: (a) 2011 HW, (b) 2012 LW, (c) 2013 HW, (d) 2014 LW, (e) 2016 LW. Orange background indicates HW conditions, blue background—LW.

Correlation analyses were also applied to the datasets to check possible correlations between metal partitioning, river Q (m³/s), suspended matter R (kg/s) discharges, sediment concentrations SSC (mg/L), average grain size D₀ (mm), as well as various grain size measures (<1 μm and <10 μm of total sample volume). We revealed that C_{susp,%} is mainly related to R and SSC at different spatial scales of the catchments, which is reflected by a high correlation coefficient *r* (*r* > 0.7) for certain metals (Table 2). Due to noticeable spatial variations in the particle size composition, the SSC within the study basins, which reflects the particle size of the sediment sources and their spatial variation, and the selectivity of the sediment mobilization and delivery processes, the driven factors were significantly varied. Thus the observed heterogeneity in partitioning patterns can be further explained by scaling in suspended sediment transport processes which is regarded as the key law in suspended sediment patterns over continental scales [88,89].

Table 2. High correlations (*r* > 0.7) C_{susp,%} revealed for certain sub-catchments of the Selenga River basin with dominant drivers of metal partitioning.

Object of Study	Number of Samples (n)	Q, (m ³ /s)	R, (kg/s)	SSC, (mg/L)	D < 1 μm	D < 10 μm	D ₀ , (mm)
Selenga basin	440	–	Ni, V, Cr, As, U, Sb	Zn, W, Sn, As, U, Sb	Fe, W	Fe, Pb, Sb, B	–
Mongolian rivers	144	–	Fe, Mn, Cr, As, U, B	Fe, Mn, Cr, As, U	–	–	–
Tuul basin	49	Cr, Sn	Ni, W, Cu, Sn, As, U, B	Zn, W, Sn, As, U, Sb	Fe, Pb, Bi	Fe, As, Sb, B	Fe, Cu

Here Q stands for water discharge, R—suspended sediment discharge, SSC—suspended sediment concentrations, D—grain size, D₀—average grain size.

Inclusion of metals into the particular box of Table 2 reveals that for the particular seasons (lines) metal demonstrate high correlation ($r > 0.7$) with the given driver (columns).

To obtain a more general overview on main drivers that define metal partitioning in the Selenga basin, PCA was applied on the whole database. Four meaningful principal components or factors with eigenvalues >1 were extracted after Varimax raw rotation for the $C_{susp,\%}$ data set. These four components explained 69.2% of the variance in the spatiotemporal distribution of $C_{susp,\%}$ values (Supplementary Material, Table S8).

The first factor was responsible for 45% of data variance and combined crustal metals that migrate mostly in suspended form: Fe–Pb–Ni–Mn–Co (Supplementary Material, Table S8). Cu with a factor loading of 0.62 could also be attributed to this association. For Fe, Mn and Pb significant correlations with amount of suspended particles in the watercourse were revealed (Table 2).

Factor 2 consists of active water migrants Mo–Sb and As with moderate connection (factor loading = 0.53; Supplementary Material, Table S8). These metals prevail in the dissolved form regardless of any hydrological conditions and the influence of anthropogenic factors. The main sources of Mo–Sb(–As) association are mining areas within the Selenga basin [40].

Factor 3 (Supplementary Material, Table S8) combines crustal metals Bi–V and less certain mining indicators Cd–W–Cr (factor loadings = 0.57 – 0.61). The share of the suspended form for Bi–V(–Cd–W–Cr) association varies significantly (excluding Bi) depending on amount of precipitation, water discharge and distance to its anthropogenic source (Supplementary Material, Table S2).

Factor 4 (Supplementary Material, Table S8) accounts for B and partly for U (factor loading = 0.62). Those metals are connected with metallogenic specialization of parent rocks in Mongolia [40] and could be found mostly in the dissolved form.

Furthermore, we summarized average patterns of metal partitioning for low water (LW) and high water (HW) seasons for the entire database and human impacted rivers (Table 3). The average trends of metal partitioning in the Selenga basin (Table 3) showed significant differences between HW and LW periods. During HW periods (field campaigns of 2013, 2014, and 2016) the share of suspended Fe, Mn, Pb, Co, Bi, and Ni was between 62–99%, while in LW periods (field campaigns of 2011, 2012, and 2015) the share of suspended forms of all metals decreased greatly due to a distinct decline of bank and soil surface erosion, as well as resuspension processes.

Table 3. Average trends of metal partitioning in the Selenga basin.

Basin Part	Season (N of Samples)	Metal Partitioning *
Average	HW ($n = 208$)	Fe ₉₈ Mn ₉₇ Pb ₉₁ Co ₈₇ Ni ₇₆ Bi ₇₁ V ₆₁ Cr ₄₈ W ₄₈ Cd ₄₇ Sn ₄₅ Cu ₄₂ As ₂₄ Zn ₂₁ Sb ₁₇ B ₇ U ₆ Mo ₂
	LW ($n = 191$)	Bi ₇₈ Fe ₆₇ Co ₅₃ Mn ₄₉ V ₄₈ Pb ₄₇ Ni ₄₁ Cu ₃₃ Cr ₂₅ Cd ₂₄ W ₂₃ Sn ₂₁ Zn ₂₀ As ₁₉ B ₁₈ U ₅ Mo ₅ Sb ₁
Areas with high anthropogenic impact	HW ($n = 18$)	Fe ₉₉ Mn ₉₅ Pb ₉₃ Bi ₈₅ Co ₈₂ Cr ₇₄ Sn ₇₃ V ₆₆ Ni ₆₂ Cu ₄₇ Zn ₄₃ W ₄₀ As ₃₁ Sb ₁₈ U ₈ B ₄ Mo ₂
	LW ($n = 18$)	Fe ₈₁ Bi ₆₃ Pb ₅₇ Cu ₅₃ Zn ₅₀ Mn ₄₉ V ₄₃ Co ₄₁ Ni ₃₁ Cd ₁₉ Cr ₁₈ W ₁₇ As ₁₀ B ₃ U ₂ Mo ₁ Sb _{0.3}

* Font color indicates the share of suspended forms of metals $>75\%$, $75-50\%$, $50-25\%$, $<25\%$.

Despite the significant differences in the quantitative indicators of the metal partitioning, three groups of metals are quite still clearly distinguished. The first group includes Fe, Mn, Bi, Pb, Co, for which, regardless of the hydroclimatic conditions and anthropogenic impact, the major form in river waters is suspended (S-metals according to K_d values). These metals belong to Factor 1–Fe–Pb–Ni–Mn–Co(–Cu) crustal and Factor 3–Bi–V(–Cd–W–Cr) crustal-mining associations. On the contrary, for Mo, B, Sb, U, As in almost all cases the predominant form of migration is dissolved (D-metals with $K_d \leq 0.1$ and As with $K_d = 0.3$). These are metals from Factor 2–Mo–Sb(–As) mining and Factor 4–B(–U) Mongolian metallogenic associations. The third group includes all other metals whose partitioning is most dependent on hydroclimatic and anthropogenic drivers (S,D-metals).

4. Conclusions

Our synthesis of high spatio-temporal resolution data from the large Selenga River basin demonstrates the importance of flood events for metal transport at the basin scale. The spatial

distribution of high and low water conditions within a large catchment, e.g., as a result of on-going flood propagation, is a main driver of metal partitioning. Overall, low-flow conditions were shown to lead to increases in the dissolved phase of metal transport, whereas high-flow conditions increased suspended transport of metals. In the Selenga River delta, metal partitioning changed slightly during the year. This is associated with (i) an intra-annual redistribution of discharge among the river channels of the delta, (ii) a decrease in the hydrodynamic activity of the flow in comparison with upstream reaches, and (iii) a seasonal pattern in the deposition of the suspended sediments in the floodplain and in the delta channels. These results highlight that over large river basins, like the Selenga, hydrological variability is a main driver of the heterogeneous patterns of metal partitioning seen across scale and time. Projected hydroclimatic changes in the investigated region, and many other regions, may impact and potentially enhance such heterogeneity. Hydrological variability across space and time is thus important to consider, both in relation to management decisions and for modeling efforts at the basin scale.

Another dominant pattern of metal partitioning shown in this study was the increase in the dissolved transport in downstream parts of the river system. This is mostly due to the fact that the upstream basin parts showed highly turbid waters due to mining activities and urban settlements. Such activities are not as wide-spread in the downstream parts, which decreased the turbidity and increased (at least in relative terms) the dissolved phase transport. For instance, in the Tuul basin, anthropogenic influence manifested in an increase in the share of suspended Cr, Zn, Ni, Cu, Cd, Be, Pb, Al, Mn, and Co downstream of the Ulaanbaatar city, and Be, Mn, Co, Zn, V, Ni, and Cd downstream of Zaamar. In the Orkhon basin downstream of the confluence with the Tuul River, the share of the suspended Cr, As, Zn, Be, U, V, Cd, Ni, Pb, Co, Al, Mo, Fe, B, Mn, Cu, and Sn forms also increased. In the Kharaa River downstream of the confluence with the Boroo River, the share of suspended Zn, Cu, Cr, and As increased due to disturbances from Boroo gold mining fields.

Notably, cities considerably impacted the amount of metals in suspension. For instance, in the Tuul River downstream of the Ulaanbaatar city untreated wastewaters increased suspended sediment concentrations by more than 300 mg/L. These anthropogenic effects on metal partitioning are however also governed by hydroclimatic conditions. For example, a domination of dissolved forms was seen during winter low flow, when the river system was covered by ice. The concentration of suspended sediments in the rivers of the Selenga River basin was then less than 3 mg/L with a few exceptions. However, local hot spot regions (just downstream of cities), which remained unfrozen, caused sharp increases in the transport of suspended metals. Such enhanced suspended metal transport could prevail for more than 20 km downstream of the hot spots. This highlights the large-scale impact of local anthropogenic activities during low flow conditions.

Despite the fact that the presented novel results were based on a few simplifying assumptions (e.g., low relative contribution of bed load transport to the total mass flows of investigated substances), which in parallel work were shown to be valid for the Selenga River basin, except for its very downstream parts; the applied methodological approach is likely relevant for large-scale investigations of water-sediment geochemistry in other regions too. Although (region-specific) accuracy and limitations of the approach would need further addressing in future research.

Supplementary Materials: The following are available online at <http://www.mdpi.com/2073-4441/12/9/2392/s1>, Table S1: Basin-wide and local studies documenting spatial changes of metal partitioning for river basins: overview. Table S2: Metals partitioning in the Selenga River basin during different years and hydrological seasons (HW—high water, LW—low water). Median values. Table S3: Metal partitioning in the Tuul River basin (median values). Table S4: Metal partitioning in the Kharaa River basin (median values). Table S5: Metals partitioning in the Orkhon River basin (median values). Table S6: Metal partitioning in the Dzhida and Modonkul rivers basins (median values). Table S7: Metal partitioning in the Uda River basin (median values). Table S8: PCA results. Factor loadings of metal partitioning ($C_{susp,\%}$ values) in the Selenga River basin.

Author Contributions: N.K. provided a general supervision of the project; G.S., M.L. and N.K. prepared original draft; J.J., J.T., G.S. and S.C. provided a text edits and improvements; G.S. also provided results and discussion of PCA; M.P. helped with visualization and hydrological data processing. All authors have read and agreed to the published version of the manuscript.

Funding: Field studies were done under support of Russian Foundation for Basic Research (RFBR 17-29-05027). Analytical work was done under support of joint project of RFBR and Russian Geographical Society (RFBR 17-05-41174—RGS). Methodical work on metal partitioning was supported by Russian Science Foundation (project 19-77-30004).

Acknowledgments: Authors thanks all members of Faculty of Geography of LMSU who participated in the field studies or performed analytical work. Authors are grateful for Irina Peters (Texas, USA) for language editing. Research was done with technical support of the Joint Russian–Mongolian complex biological expedition and Baikal Institute of Nature Management Siberian branch of the Russian Academy of sciences (BINM SB RAS).

Conflicts of Interest: The authors declare no conflict of interest. The funders had no role in the design of the study; in the collection, analyses, or interpretation of data; in the writing of the manuscript, or in the decision to publish the results.

References

1. Duarte, B.; Silva, G.; Costa, J.L.; Medeiros, J.P.; Azeda, C.; Sá, E.; Metelo, I.; Costa, M.J.; Caçador, I. Heavy metal distribution and partitioning in the vicinity of the discharge areas of Lisbon drainage basins (Tagus Estuary, Portugal). *J. Sea Res.* **2014**, *93*, 101–111. [[CrossRef](#)]
2. Taghinia Hejabi, A.; Basavarajappa, H.T.; Karbassi, A.R.; Monavari, S.M. Heavy metal pollution in water and sediments in the Kabini River, Karnataka, India. *Environ. Monit. Assess.* **2011**, *182*, 1–13. [[CrossRef](#)] [[PubMed](#)]
3. Yang, Z.; Wang, Y.; Shen, Z.; Niu, J.; Tang, Z. Distribution and speciation of heavy metals in sediments from the mainstream, tributaries, and lakes of the Yangtze River catchment of Wuhan, China. *J. Hazard. Mater.* **2009**, *166*, 1186–1194. [[CrossRef](#)] [[PubMed](#)]
4. Enguix González, A.; Ternero Rodríguez, M.; Jiménez Sá, J.C.; Fernández Espinosa, A.J.; Barragán de la Rosa, F.J.; González, A.E.; Rodríguez, M.T.; Sá, J.J.; Espinosa, A.F.; De La Rosa, F.B. Assessment of metals in sediments in a tributary of Guadalquivir River (Spain). Heavy metal partitioning and relation between the water and sediment system. *Water Air Soil Pollut.* **2000**, *121*, 11–29. [[CrossRef](#)]
5. Gaillardet, J.; Viers, J.; Dupré, B. Trace Elements in River Waters. In *Treatise on Geochemistry*; Elsevier: Amsterdam, The Netherlands, 2003; pp. 225–272. ISBN 9780080437514.
6. Lychagin, M.Y.; Tkachenko, A.N.; Kasimov, N.S.; Kroonenberg, S.B. Heavy Metals in the Water, Plants, and Bottom Sediments of the Volga River Mouth Area. *J. Coast. Res.* **2015**, *314*, 859–868. [[CrossRef](#)]
7. Djukić, A.; Lekić, B.; Rajaković-Ognjanović, V.; Veljović, D.; Vulić, T.; Djolić, M.; Naunovic, Z.; Despotović, J.; Prodanović, D. Further insight into the mechanism of heavy metals partitioning in stormwater runoff. *J. Environ. Manag.* **2016**, *168*, 104–110. [[CrossRef](#)]
8. Brick, C.M.; Moore, J.N. Diel Variation of Trace Metals in the Upper Clark Fork River, Montana. *Environ. Sci. Technol.* **1996**, *30*, 1953–1960. [[CrossRef](#)]
9. Ollivier, P.; Radakovitch, O.; Hamelin, B. Major and trace element partition and fluxes in the Rhône River. *Chem. Geol.* **2011**, *285*, 15–31. [[CrossRef](#)]
10. Bradley, S.B. Flood effects on the transport of heavy metals. *Int. J. Environ. Stud.* **1984**, *22*, 225–230. [[CrossRef](#)]
11. Barber, L.B.; Paschke, S.S.; Battaglin, W.A.; Douville, C.; Fitzgerald, K.C.; Keefe, S.H.; Roth, D.A.; Vajda, A.M. Effects of an Extreme Flood on Trace Elements in River Water—From Urban Stream to Major River Basin. *Environ. Sci. Technol.* **2017**, *51*, 10344–10356. [[CrossRef](#)]
12. Chen, J.; Bouchez, J.; Gaillardet, J.; Louvat, P. Behaviors of Major and Trace Elements During Single Flood Event in the Seine River, France. *Procedia Earth Planet. Sci.* **2014**, *10*, 343–348. [[CrossRef](#)]
13. Roussiez, V.; Probst, A.; Probst, J.-L. Significance of floods in metal dynamics and export in a small agricultural catchment. *J. Hydrol.* **2013**, *499*, 71–81. [[CrossRef](#)]
14. Censi, P.; Spoto, S.E.; Saiano, F.; Sprovieri, M.; Mazzola, S.; Nardone, G.; Di Geronimo, S.I.; Punturo, R.; Ottonello, D. Heavy metals in coastal water systems. A case study from the northwestern Gulf of Thailand. *Chemosphere* **2006**, *64*, 1167–1176. [[CrossRef](#)] [[PubMed](#)]
15. Jain, C.K.; Singhal, D.C.; Sharma, M.K. Metal Pollution Assessment of Sediment and Water in the River Hindon, India. *Environ. Monit. Assess.* **2005**, *105*, 193–207. [[CrossRef](#)] [[PubMed](#)]
16. Wang, W.; Wang, W.-X. Phase partitioning of trace metals in a contaminated estuary influenced by industrial effluent discharge. *Environ. Pollut.* **2016**, *214*, 35–44. [[CrossRef](#)] [[PubMed](#)]

17. Karbassi, A.R.; Fakhraee, M.; Heidari, M.; Vaezi, A.R.; Valikhani Samani, A.R. Dissolved and particulate trace metal geochemistry during mixing of Karganrud River with Caspian Sea water. *Arab. J. Geosci.* **2015**, *8*, 2143–2151. [[CrossRef](#)]
18. Shafer, M.M.; Overdier, J.T.; Hurley, J.P.; Armstrong, D.; Webb, D. The influence of dissolved organic carbon, suspended particulates, and hydrology on the concentration, partitioning and variability of trace metals in two contrasting Wisconsin watersheds (USA). *Chem. Geol.* **1997**, *136*, 71–97. [[CrossRef](#)]
19. Islam, M.S.; Ahmed, M.K.; Raknuzzaman, M.; Habibullah -Al- Mamun, M.; Islam, M.K. Heavy metal pollution in surface water and sediment: A preliminary assessment of an urban river in a developing country. *Ecol. Indic.* **2015**, *48*, 282–291. [[CrossRef](#)]
20. Gallo, M.; Trento, A.; Alvarez, A.; Beldoménico, H.; Campagnoli, D. Dissolved and Particulate Heavy Metals in the Salado River (Santa FE, Argentina). *Water Air Soil Pollut.* **2006**, *174*, 367–384. [[CrossRef](#)]
21. Nadmitov, B.; Hong, S.; In Kang, S.; Chu, J.M.; Gomboev, B.; Janchivdorj, L.; Lee, C.-H.; Khim, J.S. Large-scale monitoring and assessment of metal contamination in surface water of the Selenga River Basin (2007–2009). *Environ. Sci. Pollut. Res.* **2015**, *22*, 2856–2867. [[CrossRef](#)]
22. Zhang, Z.; Wang, J.J.; Ali, A.; DeLaune, R.D. Heavy metal distribution and water quality characterization of water bodies in Louisiana’s Lake Pontchartrain Basin, USA. *Environ. Monit. Assess.* **2016**, *188*. [[CrossRef](#)] [[PubMed](#)]
23. Chalov, S.R.; Liu, S.; Chalov, R.S.; Chalova, E.R.; Chernov, A.V.; Promakhova, E.V.; Berkovitch, K.M.; Chalova, A.S.; Zavadsky, A.S.; Mikhailova, N. Environmental and human impacts on sediment transport of the largest Asian rivers of Russia and China. *Environ. Earth Sci.* **2018**, *77*, 274. [[CrossRef](#)]
24. Viers, J.; Dupré, B.; Gaillardet, J. Chemical composition of suspended sediments in World Rivers: New insights from a new database. *Sci. Total Environ.* **2009**, *407*, 853–868. [[CrossRef](#)] [[PubMed](#)]
25. Dupré, B.; Gaillardet, J.; Rousseau, D.; Allègre, C.J. Major and trace elements of river-borne material: The Congo Basin. *Geochim. Cosmochim. Acta* **1996**, *60*, 1301–1321. [[CrossRef](#)]
26. Guéguen, C.; Dominik, J. Partitioning of trace metals between particulate, colloidal and truly dissolved fractions in a polluted river: The Upper Vistula River (Poland). *Appl. Geochem.* **2003**, *18*, 457–470. [[CrossRef](#)]
27. Myangan, O.; Kawahigashi, M.; Oyuntsetseg, B.; Fujitake, N. Impact of land uses on heavy metal distribution in the Selenga River system in Mongolia. *Environ. Earth Sci.* **2017**, *76*, 346. [[CrossRef](#)]
28. Chalov, S.; Moreido, V.; Sharapova, E.; Efimova, L.; Efimov, V.; Lychagin, M.; Kasimov, N. Hydrodynamic controls of particulate metals partitioning along the lower Selenga River—Main tributary of the Lake Baikal. *Water* **2020**, *12*, 1345. [[CrossRef](#)]
29. Chalov, S.; Thorslund, J.; Kasimov, N.; Aybullatov, D.; Ilyicheva, E.; Karthe, D.; Kositsky, A.; Lychagin, M.; Nitrouer, J.; Pavlov, M.; et al. The Selenga River delta: A geochemical barrier protecting Lake Baikal waters. *Reg. Environ. Change* **2017**, *17*, 2039–2053. [[CrossRef](#)]
30. Thorslund, J.; Jarsjö, J.; Wällstedt, T.; Mörth, C.M.; Lychagin, M.Y.; Chalov, S.R. Geochemical controls on the partitioning and hydrological transport of metals in a non-acidic river system. *Hydrol. Earth Syst. Sci. Discuss.* **2014**, *11*, 9715–9758. [[CrossRef](#)]
31. Thorslund, J.; Jarsjö, J.; Wällstedt, T.; Mörth, C.M.; Lychagin, M.Y.; Chalov, S.R. Speciation and hydrological transport of metals in non-acidic river systems of the Lake Baikal basin: Field data and model predictions. *Reg. Environ. Change* **2017**, *17*, 2007–2021. [[CrossRef](#)]
32. Kasimov, N.; Karthe, D.; Chalov, S. Environmental change in the Selenga River—Lake Baikal Basin. *Reg. Environ. Change* **2017**, *17*, 1945–1949. [[CrossRef](#)]
33. Chalov, S.S.R.; Jarsjö, J.; Kasimov, N.S.N.S.; O Romanchenko, A.; Pietroń, J.; Thorslund, J.; Promakhova, E.V.E.V.; Romanchenko, A.; Pietroń, J.; Thorslund, J.; et al. Spatio-temporal variation of sediment transport in the Selenga River Basin, Mongolia and Russia. *Environ. Earth Sci.* **2014**, *73*, 663–680. [[CrossRef](#)]
34. Moatar, F.; Meybeck, M.; Raymond, S.; Birgand, F.; Curie, F. River flux uncertainties predicted by hydrological variability and riverine material behaviour. *Hydrol. Process.* **2013**, *27*, 3535–3546. [[CrossRef](#)]
35. Rode, M.; Suhr, U. Uncertainties in selected river water quality data. *Hydrol. Earth Syst. Sci. Discuss.* **2007**, *11*, 863–874. [[CrossRef](#)]
36. Horowitz, A. *A Primer on Trace Metal-Sediment Chemistry*; US Government Printing Office: Alexandria, VA, USA, 1985.

37. Robertson, D.M.; Roerish, E.D. Influence of various water quality sampling strategies on load estimates for small streams. *Water Resour. Res.* **1999**, *35*, 3747–3759. [[CrossRef](#)]
38. Littlewood, I. Hydrological regimes, sampling strategies, and assessment of errors in mass load estimates for United Kingdom rivers. *Environ. Int.* **1995**, *21*, 211–220. [[CrossRef](#)]
39. Birgand, F.; Fauchoux, C.; Gruau, G.; Moatar, F.; Meybeck, M. Uncertainties in Assessing Annual Nitrate Loads and Concentration Indicators: Part 2. Deriving Sampling Frequency Charts in Brittany, France. *Trans. ASABE* **2011**, *54*, 93–104. [[CrossRef](#)]
40. Kasimov, N.; Shinkareva, G.; Lychagin, M.; Kosheleva, N.; Chalov, S.; Pashkina, M.; Thorslund, J.; Jarsjö, J. River water quality of the Selenga-Baikal basin: Part I—Spatio-temporal patterns of dissolved and suspended metals. *Water* **2020**, *12*, 2137. [[CrossRef](#)]
41. Shabanova, E.V.; Byambasuren, T.; Ochirbat, G.; Vasil'eva, I.E.; Khuukhenkhuu, B.; Korolkov, A.T. Relationship between major and trace elements in Ulaanbaatar soils: A study based on multivariate statistical analysis. *Geogr. Environ. Sustain.* **2019**, *12*, 199–212. [[CrossRef](#)]
42. Aschmann, M. Addressing air pollution and beyond in Ulaanbaatar: The role of sustainable mobility. *Geogr. Environ. Sustain.* **2019**, *12*, 213–223. [[CrossRef](#)]
43. Garmaev, E.Z.; Kulikov, A.I.; Tsydyrov, B.Z.; Sodnomov, B.V.; Ayurzhanayev, A.A. Environmental conditions of Zakamensk town (Dzhida River basin Hotspot). *Geogr. Environ. Sustain.* **2019**, *12*, 224–239. [[CrossRef](#)]
44. Gradel, A.; Sukhbaatar, G.; Karthe, D.; Kang, H. Forest management in Mongolia—A review of challenges and lessons learned with special reference to degradation and deforestation. *Geogr. Environ. Sustain.* **2019**, *12*, 133–166. [[CrossRef](#)]
45. Aitrell, D. Multipurpose national forest inventory in Mongolia, 2014–2017—A tool to support sustainable forest management. *Geogr. Environ. Sustain.* **2019**, *12*, 167–183. [[CrossRef](#)]
46. Thorslund, J.; Chalov, S.; Karthe, D.; Jarsjö, J. Impacts of hydroclimate and mining on arsenic contamination of groundwater and surface water systems in Central Asia. In Proceedings of the Sixth International Congress on Arsenic in the Environment (As2016), Stockholm, Sweden, 19–23 June 2016; CRC Press: Boca Raton, FL, USA; pp. 185–186. [[CrossRef](#)]
47. Batsaikhan, B.; Kwon, J.S.; Kim, K.H.; Lee, Y.J.; Lee, J.H.; Badarch, M.; Yun, S.T. Hydrochemical evaluation of the influences of mining activities on river water chemistry in central northern Mongolia. *Environ. Sci. Pollut. Res.* **2017**. [[CrossRef](#)] [[PubMed](#)]
48. Juříčka, D.; Pecina, V.; Brtnický, M.; Kynický, J. Mining as a catalyst of overgrazing resulting in risk of forest retreat, Erdenet Mongolia. *Geogr. Environ. Sustain.* **2019**, *12*, 184–198. [[CrossRef](#)]
49. Gelfan, A.N.; Millionshchikova, T.D. Validation of a Hydrological Model Intended for Impact Study: Problem Statement and Solution Example for Selenga River Basin. *Water Resour.* **2018**, *45*, 90–101. [[CrossRef](#)]
50. Frolova, N.L.; Belyakova, P.A.; Grigoriev, V.Y.; Sazonov, A.A.; Zotov, L.V.; Jarsjö, J. Runoff fluctuations in the Selenga River Basin. *Reg. Environ. Change* **2017**, *17*, 1965–1976. [[CrossRef](#)]
51. Kaus, A.; Schäffer, M.; Büttner, O.; Karthe, D.; Borchardt, D. Regional patterns of heavy metal concentrations in water, sediment and five consumed fish species of the Kharaa River basin, Mongolia. *Reg. Environ. Change* **2016**. [[CrossRef](#)]
52. Karthe, D.; Kasimov, N.S.; Chalov, S.R.; Shinkareva, G.L.; Malsy, M.; Menzel, L.; Theuring, P.; Hartwig, M.; Schweitzer, C.; Hofmann, J.; et al. Integrating multi-scale data for the assessment of water availability and quality in the Kharaa-Orkhon-Selenga river system. *Geogr. Environ. Sustain.* **2014**, *7*, 65–86. [[CrossRef](#)]
53. Kasimov, N.; Kosheleva, N.; Lychagin, M.; Chalov, S.; Alexeenko, A.; Bazilova, V.; Beshentsev, A.; Bogdanova, M.; Chernov, A.; Dorjgotov, D.; et al. *Environmental Atlas-Monograph “Selenga-Baikal”*; Kasimov, N., Kosheleva, N., Lychagin, M., Chalov, S., Eds.; Faculty of Geography of Lomonosov Moscow State University: Moscow, Russia, 2019; ISBN 978-5-9500502-4-4.
54. Warren, L.A.; Zimmerman, A.P. The influence of temperature and NaCl on cadmium, copper and zinc partitioning among suspended particulate and dissolved phases in an urban river. *Water Res.* **1994**, *28*, 1921–1931. [[CrossRef](#)]
55. Benoit, G.; Rozan, T.F. The influence of size distribution on the particle concentration effect and trace metal partitioning in rivers. *Geochim. Cosmochim. Acta* **1999**, *63*, 113–127. [[CrossRef](#)]
56. Kasimov, N.S.; Lychagin, M.Y.; Chalov, S.R.; Shinkareva, G.L. Paragenetic associations of chemical elements in landscapes. *Vestn. Mosk. Univ. Ser. 5 Geogr.* **2019**, *6*, 20–28.

57. Pietroń, J.; Chalov, S.R.; Chalova, A.S.; Alekseenko, A.V.; Jarsjö, J. Extreme spatial variability in riverine sediment load inputs due to soil loss in surface mining areas of the Lake Baikal basin. *CATENA* **2017**, *152*, 82–93. [[CrossRef](#)]
58. Altansukh, O.; Davaa, G. Application of Index Analysis to Evaluate the Water Quality of the Tuul River in Mongolia. *J. Water Resour. Prot.* **2011**. [[CrossRef](#)]
59. Batbayar, Z.; Dolgorsuren, G.; Bron, J.; Dolgorsuren, G.; Chagnaa, N.; Gerelchuluun, J.; Puntsagsuren, C.; van der Linden, W. *Tuul River Basin Integrated Water Management Plan*; Preprint; Sh.Gantuul: Ulaanbaatar, Mongolia, 2012.
60. Byambaa, B.; Todo, Y. Impact of placer gold mine technology on water quality: A case study of Tuul river valley in the Zaamar goldfield, Mongolia. In *Proceedings of the Water Resources Management VI*; WIT Press: Southampton, UK, 2011; pp. 309–318.
61. Lee, Y.J.; Yun, S.T.; Badarch, M.; Lee, J.; Ayur, O.; Kwon, J.S.; Kim, D.M. *Joint Research between Korea and Mongolia on Water Quality and Contamination of Transboundary Watershed in Northern Mongolia*; Korea Environmental Institute, Mongolian Nature and Environment Consortium, Mongolia: Seoul, Korea, 2006; ISBN 978-89-8464-214-0 93530.
62. Sato, H. Mongolia: the water situation in Ulaanbaatar. *Soc. Syst. Rev.* **2012**, *3*, 55–63.
63. Odontsetseg, D.; Janchivdorj, L.; Udvaltsetseg, G.; Frieden, J. Some Results of Applying DPSIR Analysis for Ulaanbaatar as Part of the Selenge River Basin Integrated Water Management System. *Proc. Mong. Acad. Sci.* **2011**, 22–31. [[CrossRef](#)]
64. Altansukh, O. A Spatio-Temporal Assessment of the Water Quality in Tuul River, Mongolia. *Mong. J. Biol. Sci.* **2009**, *7*, 51–59. [[CrossRef](#)]
65. Sikder, M.T.; Kihara, Y.; Yasuda, M.; Mihara, Y.; Tanaka, S.; Odgerel, D.; Mijiddorj, B.; Syawal, S.M.; Hosokawa, T.; Saito, T.; et al. River Water Pollution in Developed and Developing Countries: Judge and Assessment of Physicochemical Characteristics and Selected Dissolved Metal Concentration. *CLEAN Soil Air Water* **2013**, *41*, 60–68. [[CrossRef](#)]
66. Dalai, B.; Ishiga, H. Geochemical evaluation of present-day Tuul River sediments, Ulaanbaatar basin, Mongolia. *Environ. Monit. Assess.* **2013**, *185*, 2869–2881. [[CrossRef](#)]
67. Sorokina, O.I.; Kosheleva, N.E.; Kasimov, N.S.; Golovanov, D.L.; Bazha, S.N.; Dorzhgotov, D.; Enkh-Amgalan, S. Heavy metals in the air and snow cover of Ulan Bator. *Geogr. Nat. Resour.* **2013**, *34*, 291–301. [[CrossRef](#)]
68. Kosheleva, N.; Kasimov, N.; Dorjgotov, D.; Bazha, S.; Golovanov, D.; Sorokina, O.; Enkh-Amgalan, S. Assessment of heavy metal pollution of soils in industrial cities of Mongolia. *Geogr. Environ. Sustain.* **2010**, *3*, 51–65. [[CrossRef](#)]
69. Batjargal, T.; Otgonjargal, E.; Baek, K.; Yang, J.-S. Assessment of metals contamination of soils in Ulaanbaatar, Mongolia. *J. Hazard. Mater.* **2010**, *184*, 872–876. [[CrossRef](#)] [[PubMed](#)]
70. Kasimov, N.S.; Kosheleva, N.E.; Sorokina, O.I.; Bazha, S.N.; Gunin, P.D.; Enkh-Amgalan, S. Ecological-geochemical state of soils in Ulaanbaatar (Mongolia). *Eurasian Soil Sci.* **2011**, *44*, 709–721. [[CrossRef](#)]
71. Thorslund, J.; Jarsjö, J.; Chalov, S.R.; Belozero, E.V. Gold mining impact on riverine heavy metal transport in a sparsely monitored region: The upper Lake Baikal Basin case. *J. Environ. Monit.* **2012**, *14*, 2780. [[CrossRef](#)]
72. Inam, E.; Khantotong, S.; Kim, K.-W.; Tumendemberel, B.; Erdenetsetseg, S.; Puntsag, T. Geochemical distribution of trace element concentrations in the vicinity of Boroo gold mine, Selenge Province, Mongolia. *Environ. Geochem. Health* **2011**, *33*, 57–69. [[CrossRef](#)]
73. Pfeiffer, M.; Batbayar, G.; Hofmann, J.; Siegfried, K.; Karthe, D.; Hahn-Tomer, S. Investigating arsenic (As) occurrence and sources in ground, surface, waste and drinking water in northern Mongolia. *Environ. Earth Sci.* **2015**, *73*, 649–662. [[CrossRef](#)]
74. Hofmann, J.; Watson, V.; Scharaw, B. Groundwater quality under stress: Contaminants in the Kharaa River basin (Mongolia). *Environ. Earth Sci.* **2015**, *73*, 629–648. [[CrossRef](#)]
75. Theuring, P.; Rode, M.; Behrens, S.; Kirchner, G.; Jha, A. Identification of fluvial sediment sources in the Kharaa River catchment, Northern Mongolia. *Hydrol. Process.* **2013**, *27*, 845–856. [[CrossRef](#)]
76. Hofmann, J.; Hürdler, J.; Ibisch, R.; Schaeffer, M.; Borchardt, D. Analysis of Recent Nutrient Emission Pathways, Resulting Surface Water Quality and Ecological Impacts under Extreme Continental Climate: The Kharaa River Basin (Mongolia). *Int. Rev. Hydrobiol.* **2011**, *96*, 484–519. [[CrossRef](#)]

77. Karthe, D.; Heldt, S.; Houdret, A.; Borchardt, D. IWRM in a country under rapid transition: Lessons learnt from the Kharaa River Basin, Mongolia. *Environ. Earth Sci.* **2015**, *73*, 681–695. [[CrossRef](#)]
78. Karthe, D.; Borchardt, D.; Kaus, A. Towards an integrated water resources management for the Kharaa catchment, Mongolia. In Proceedings of the IWA 1st Central Asian Regional Young and Senior Water Professionals Conference, Almaty, Kazakhstan, 22–24 September 2011; pp. 79–93.
79. Alekseevskii, N.I.; Bezozerova, E.V.; Kasimov, N.S.; Chalov, S.R. Spatial variability of suspended sediment transport characteristics in the Selenga Basin during rain floods. *Vestn. Mosk. Univ. Ser. Geogr.* **2013**, *3*, 60–65.
80. Timofeev, I.V.; Kosheleva, N.E.; Kasimov, N.S.; Gunin, P.D.; Sandag, E.-A. Geochemical transformation of soil cover in copper–molybdenum mining areas (Erdenet, Mongolia). *J. Soils Sediments* **2015**, *16*, 1225–1237. [[CrossRef](#)]
81. Tarmakhanov, E.E.; Budaev, D.A. The coal industry of Buryatia in 1960–1991. *Bull. Buryat State Univ. Pedagog. Philol. Philos. Russ.* **2015**, 48–51. [[CrossRef](#)]
82. Verkhoturov, A.G.; Razmakhnina, I.B. Geological engineering problems in the development of coal deposits in the Trans-Baikal Territory. *Bull. Transbaikal State Univ. Russ.* **2015**, *8*, 123.
83. Kasimov, N.S.; Korlyakov, I.D.; Kosheleva, N.E. Distribution and factors of accumulation of heavy metals and metalloids in river bottom sediments in the territory of the Ulan-Ude city. *Rudn. J. Ecol. Life Saf.* **2017**, *25*, 380–395. [[CrossRef](#)]
84. Tansel, B.; Rafiuddin, S. Heavy metal content in relation to particle size and organic content of surficial sediments in Miami River and transport potential. *Int. J. Sediment. Res.* **2016**, *31*, 324–329. [[CrossRef](#)]
85. Promakhova, E.V. Variability of River Water Turbidity in Different Phases of the Water Regime. Ph.D. Thesis, Lomonosov Moscow State University, Moscow, Russia, 19 May 2016.
86. Pietroń, J.; Nittrouer, J.A.; Chalov, S.R.; Dong, T.Y.; Kasimov, N.; Shinkareva, G.; Jarsjö, J. Sedimentation patterns in the Selenga River delta under changing hydroclimatic conditions. *Hydrol. Process.* **2018**, *32*, 278–292. [[CrossRef](#)]
87. Bouchez, J.; Gaillardet, J.; France-Lanord, C.; Maurice, L.; Dutra-Maia, P. Grain size control of river suspended sediment geochemistry: Clues from Amazon River depth profiles. *Geochem. Geophys. Geosyst.* **2011**, *12*, Q03008. [[CrossRef](#)]
88. Church, M. Interpreting sediment yield scaling. *Earth Surf. Process. Landf.* **2017**, *42*, 1895–1898. [[CrossRef](#)]
89. Lu, H.; Moran, C.J.; Sivapalan, M. A theoretical exploration of catchment-scale sediment delivery. *Water Resour. Res.* **2005**, *41*, 1–15. [[CrossRef](#)]



© 2020 by the authors. Licensee MDPI, Basel, Switzerland. This article is an open access article distributed under the terms and conditions of the Creative Commons Attribution (CC BY) license (<http://creativecommons.org/licenses/by/4.0/>).